TITANATE NANOTUBES PRODUCED FROM MICROWAVE-ASSISTED HYDROTHERMAL SYNTHESIS: CHARACTERIZATION, ADSORPTION AND PHOTOCATALYTIC ACTIVITY

M. C. Manique[*], A. Posteral Silva, A. K. Alves and C. P. Bergmann

Laboratory of Ceramic Materials, Universidade Federal do Rio Grande do Sul, UFRGS,
Department of Materials, Av. Osvaldo Aranha 99/711, CEP: 90035-190, Porto Alegre - RS, Brazil.
Phone: +55 51 33083637; Fax: + 55 51 33083405
E-mail: marciamanique@yahoo.com.br

Abstract - A microwave-assisted hydrothermal (MAH) method was employed to synthesize TiO_2 nanotubes (TNTs) and these were compared to the conventional hydrothermal (CH) method. The nanotubes were characterized for their crystallinity, morphology, surface area and photocatalytic activity. The TiO_2 P25 was used for comparison purposes and efficiently degraded both dyes. However, methylene blue was adsorbed on the nanotube surfaces, which can be attributed to the electrostatic interaction between the cationic methylene blue and the negatively charged TNT surface. On the other hand, all nanotubes had a photocatalytic performance with methyl orange (anionic dye). Additional degradation was observed for nanotubes synthesized via the MAH method at 150 °C. This can be directly related to their larger surface area. Adsorption mechanisms of TNTs were also discussed by applying the Langmuir and Freundlich isotherm. The results show an efficient dye wastewater treatment through the application of TNT photocatalyst.
Keywords: Photocatalysis; Titanate nanotubes; Microwave-assisted hydrothermal synthesis; Adsorption.

INTRODUCTION

TNTs have recently received increasing attention in photocatalytic applications due to their unique physicochemical properties, including nanotubular structure with layered walls, high surface area and ion-exchange ability (Cui *et al*., 2012; Peng *et al*., 2010). The first synthesis of TNTs was reported in 1996 by Hoyer (1996) via electrochemical deposition on a molding of aluminum oxide. The template method utilizes the properties of a material known for the production of similar morphology through deposition or dissolution to produce regular and controlled nanotubes (Ku *et al*., 2013). However, this method has a high cost due to the loss of the mold at the end of the process (Bavykin *et al*., 2006).

Soon after, TNTs were produced by a hydrothermal method by Kasuga *et al*. (1998) and anodic oxidation by Zwilling *et al*. (1999). The synthesis by anodization is a process capable of forming an oxide layer on the surface of a metal, allowing the growth of highly organized TiO_2 nanotubes (Zhang *et al*., 2007). Disadvantageously, this process requires the use of toxic hydrofluoric acid solution (Liu *et al*., 2014).

The hydrothermal method is most widely used for the production of TNTs because of its simplicity and capability to produce large-area nanotubes (Cui *et al*., 2012). This process is based on the reaction of TiO_2 nanoparticles with concentrated NaOH solution at high pressures; these subsequently undergo an acid wash. This approach is simple and effective for the synthesis of nanotubes (Cui *et al*., 2012; Peng *et al*.,

---

*To whom correspondence should be addressed

2010; Huang and Chien, 2013), but does require a long reaction time (minimum of 20 h) and large amounts of energy (Peng *et al.*, 2010; Li *et al.*, 2011).

The microwave-assisted hydrothermal (MAH) system offers fast and uniform heating versus the conventional method (Li *et al.*, 2011; Wu *et al.*, 2005). This occurs because of the direct heating of nanoparticles by electromagnetic waves. This provides even and uniform growth of nanotubes (Li *et al.*, 2011; Wu *et al.*, 2005). The parameters involved in the synthesis such as reaction time and temperature were studied to understand their influence on the process of obtaining nanotubes. The temperature predominantly affects the product morphology (Chung *et al.*, 2008).

TNT exhibits immense potential in a wide variety of applications such as a support for other active elements in catalytic reactions (Macak *et al.*, 2005), as devices for dye-sensitized solar cells (Kim *et al.*, 2008), as a coating for bone and dental implants for the deposition of hydroxyapatite (Kodama *et al.*, 2009) and as photocatalyst (Lee *et al.*, 2011). However, in the photocatalytic degradation of dyestuffs, most current work utilizes P25 (Lachheb *et al.*, 2002; Stylidi *et al.*, 2003) or anodized TNT (Zhang *et al.*, 2007; Yuan *et al.*, 2009; Luan and Wang, 2014). There is a distinct lack of available information in terms of photocatalytic performance of hydrothermally-synthesized TNT.

In this paper, we describe a MAH method with higher temperatures and shorter reaction times versus the CH method for TNT synthesis. The structural properties and photocatalytic performance of the nanotubes were investigated. Moreover, the kinetics and equilibrium adsorption model were also used to fit the experimental data and adsorption mechanism of the methylene blue to the surface of TNTs.

EXPERIMENTAL

Synthesis Via the Conventional Hydrothermal Method

This procedure was based on the work of Kasuga *et al.* (1998) in which a solution was prepared with 3 g of TiO_2 (P25 Evonik) and 100 mL of 10 M NaOH and stirred for 1 h at 50 °C. The solution was then transferred to a stainless steel autoclave (Ekipar) using a Teflon bottle. The solution was magnetically stirred and heated at 110 °C and 130 °C for 20 and 48 h. Temperatures above 130 °C could not be used due to loss of balance of the internal pressure of the reactor. After the reaction, the material was washed with

deionized water and 0.1 M HCl to adjust the pH. The material was then dried for 15 hours at 80 °C. Finally, the sample was heat-treated at 450 °C for 1 h.

Synthesis by the Microwave-Assisted Hydrothermal Method

The methodology is based to the work of Peng *et al.* (2010). The samples were prepared with a microwave digestion system (MDS-8G) in Teflon-lined bottles. We added 0.6 g of TiO_2 (P25) to 70 mL of 10 M NaOH. The reactions were programmed to 400 W of power at 110 °C, 130 °C and 150 °C for 1.5 and 3 h. The post-reaction processing was the same as above.
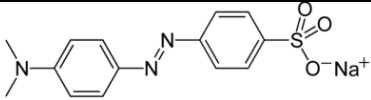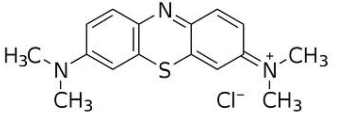
Characterization of TNTs

The morphology of the samples was analyzed by transmission electron microscopy (TEM) using a JEOL JEM 1200 EX II instrument. The specific area and pore size distribution were measured by adsorption–desorption isotherms (N_2) at 77 K using the BET (Brunauer, Emmett and Teller) and BJH (Barret, Joyner and Hallenda) methods, respectively. The analysis was performed using a Quantachrome Nova 1000e. The XRD analyses were carried out with a Philips X-ray diffractometer (model X'PERT MDP) using Ni-filtered Cu Kα radiation at 15.418 nm in the 2θ range from 5° to 75°.

Photocatalysis Assays

We used methyl orange and methylene blue whose properties are described in Table 1. The experiments were performed in a photocatalytic system consisting of a Pyrex glass-jacketed reactor exposed to air and two brackets for UV light irradiation (in the form of half-cylinders); each contained six 8 W Sylvania Blacklight blue UVA (maximum radiation at 355-360 nm; length of 28.7 cm) lamps and a magnetic stirrer. Details of the photochemical reactor have been reported elsewhere (Trommer *et al.*, 2010). The temperature of the reactor was held constant (30 ºC) by a thermostatically-controlled water circulator (Thermo Scientific). For each photocatalyst test, 50 mg of the photocatalytic material was added to 125 mL of 20 ppm dye solution. Before irradiation, the suspension was stirred in the dark for 20 minutes to reach the adsorption equilibrium of dye on the photocatalyst. Sampling was performed at stated time intervals and filtered through a Millipore filter (0.22 μm). The concentration of dye in the filtrate was determined by measuring its UV-visible absorbance using a Shimadzu RF5301PC spectrophotometer.

Table 1: Description of the dyes used in the photocatalytic degradation tests.

Dye	Molecular structure	Type	Concentration (ppm)
Methyl orange		Anionic	20
Methylene blue		Cationic	20

Methylene Blue Adsorption

The adsorption isotherms of methylene blue on the TNTs were determined using the batch process. Typically, 0.02 g of TNTs were introduced into 20 mL of dye solution in a conical flask with different initial concentrations (C_0). After continuous shaking in the dark for 12 h, the suspension was filtered and UV–visible absorbance employed to measure the residual concentration of methylene blue in the solution. The equilibrium adsorption amount (Q_e) of methylene blue was calculated according to Equation (1):

$$Q_e = \frac{(C_0 - C_e)V}{M} \qquad (1)$$

Here, Q_e is the equilibrium adsorption amount (mg/g), C_0 and C_e are the initial and equilibrium concentrations of methylene blue (mg/L), respectively, M is the mass of TNTs (g), and V is the volume of methylene blue solution (L).

RESULTS AND DISCUSSION

Characterization of the TNTs

Table 2 shows the surface area and pore volume of TNTs produced by the conventional method sintered at 110 °C for 20 h under different pH conditions.

Table 2: Surface area of the titania nanotubes synthesized by the CH method with different pH conditions.

Sample	Surface area ($m^2\,g^{-1}$)	Pore volume ($cm^3\,g^{-1}$)
CH 110-20 pH 4	64.27	0.55
CH 110-20 pH 7	53.22	0.43
CH 110-20 pH 10	49.97	0.35

The most acidic sample (pH 4) showed the highest surface area and pore volume with a gradual reduction with increasing pH. The difference in sample pore volumes, provided by the samples may be related to the amount of Na^+ ions present. The presence of Na^+ ions is not desirable because it significantly reduces the TiO_2 photocatalytic activity (Lee *et al.*, 2011). The acid wash treatment contributes to increases in surface area and pore volume by decreasing the presence of Na^+. In this step, the Na^+ are exchanged by H^+ ions, providing changes to the structure of the nanotubes.

The walls of the nanotubes are formed by titanate ($Ti_3O_7^{2-}$). This characteristic leads to the need for a cationic interlayer region to compensate for negative charges. Previously, Ferreira *et al.* (2006) suggested that the reaction of TiO_2 and NaOH forms a sodium titanate structure ($Na_2Ti_3O_7$), where the interlayer region is occupied by Na^+ ions. This difference would promote a small change in the interplanar distance with an exchange of Na^+ by H^+ after acid washing. Finally, they proposed the composition to be $Na_{2-x}H_xTi_3O_7$ where the value of x depends on the washing conditions to which the nanotubes are submitted.

According to the XRD patterns (Figure 1), the samples are anatase. However, there is a reduction in the peak intensity for the sample at pH 10. The presence of Na^+ may have affected the crystallinity of the sample and caused it to remain amorphous even after the heat treatment (Tsai and Teng, 2006). Based on these results, pH 4 was fixed for the post-treatment of the other nanotube samples.

The N_2 adsorption-desorption curves for TNT samples (Figure 2) show a typical type–IV isotherm, which is characteristic of mesoporous materials (Bavykin *et al.*, 2004). In addition, the hysteresis loop shifted to high P/Po values (>0.8), suggestive of larger mesopores in the sample. This was confirmed by the corresponding pore-size distribution (Figure 2 inset). The pore size distribution curve indicated two

sets of pores. The pore sizes below 4 nm could be attributed to the pores inside of the nanotubes, with sizes similar to the inner diameter of the nanotubes. The larger pores (ca. 20-90 nm) refer to the pores between the nanotubes (Bavykin *et al*., 2004; Huang *et al*., 2013).

The surface area and pore volume of the remaining TNTs synthesized by both methods are shown in Table 3.
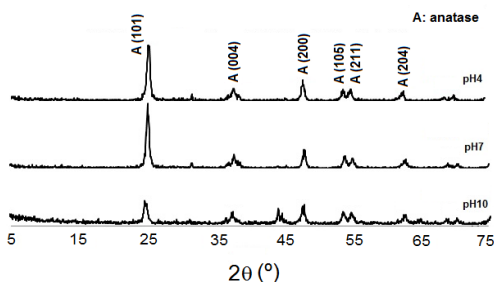

Figure 1: XRD patterns of TiO_2 nanotubes synthesized at 110 °C and 20 h (sample CH 110-20) with different pH conditions.
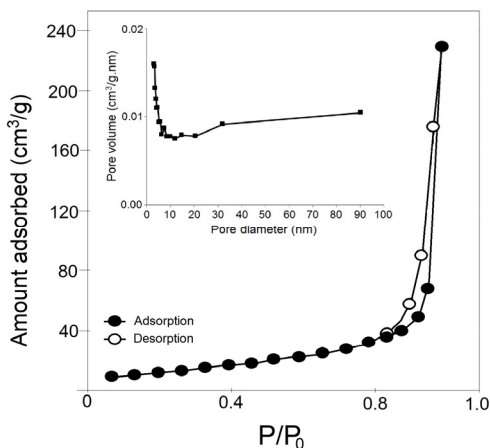

Figure 2: N_2 adsorption-desorption isotherms for CH 110-20 sample. Inset: pore volume distribution of CH 110-20.

Table 3: Comparison of the surface area of titania nanotubes and TiO_2 P25.

Method	Sample	Surface area (m² g⁻¹)	Pore volume (cm³ g⁻¹)
	TiO_2 P25	58.34	0.19
Conventional Hydrothermal	CH 110-20	64.27	0.55
	CH 110-48	41.39	0.39
	CH 130-20	48.85	0.42
	CH 130-48	36.32	0.11
Microwave-assisted Hydrothermal	MAH 110-1.5	107.05	0.56
	MAH 130-1.5	74.15	0.41
	MAH 150-1.5	111.39	0.58
	MAH 110-3	23.34	0.14
	MAH 130-3	79.78	0.45
	MAH 150-3	106.51	0.52

The samples synthesized at higher temperatures had lower surface areas and pore volumes. This decrease was more pronounced for the sample synthesized at 130 °C for 48 h. The increase in temperature and reaction time may have resulted in the formation of nanotubes with a more rigid structure, such as nanorods or nanoribbons (non-tubular particles). Nanotubes produced by microwave irradiation showed higher values for the surface area versus the values provided by the conventional method. In contrast, MAH samples 110-3 had a smaller surface area. Larger surface areas were obtained at the highest temperature (150 ºC).

Figure 3 shows the XRD patterns of the TNTs synthesized by both methods.
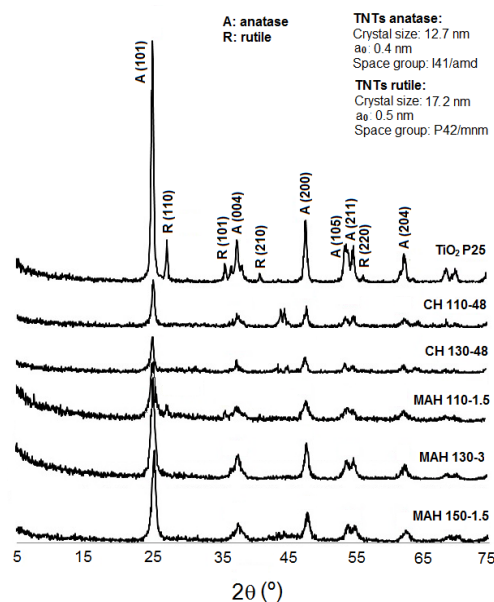

Figure 3: XRD patterns of TiO_2 P25 and TNTs synthesized by the CH and MAH methods.

From the crystallographic database and spectra, we concluded that the nanotubes have an anatase phase. There is no evidence of a rutile phase. However, for the samples synthesized at 110 °C with the MAH method, we did observe evidence of a rutile phase. This might be because of incomplete amorphization of samples at this lower temperature. This causes the crystalline phase to remain. The photocatalytic properties of TiO_2 nanoparticles are strongly dependent on the nature of the crystalline phase. The anatase phase generally exhibits a higher photocatalytic activity than the rutile phase; therefore, this is a desirable step in obtaining nanotubes.

Figure 4 shows TEM images of some TNTs samples. For CH 110-20 (Figure 4a), we observed a tubular titania morphology with diameters between 20

and 80 nm. This shows that these conditions (110 °C - 20 h) are sufficient to form nanotubes. This concurs with previous studies (Kasuga *et al.*, 1998; Yang *et al.*, 2003). We also observed the formation of filaments with diameters smaller than the nanotubes. These also show the presence of unreacted TiO_2 nanoparticles. For CH 130-48, we noted the presence of non-tubular or nanoribbon structures (Figure 4b) as reported in other studies (Bavykin *et al.*, 2004; Huang *et al.*, 2009). This explains the low surface area and pore volume presented for this sample. According to Huang *et al.* (2009), higher reaction times favor the formation of nanoribbons. This is due to dissolution of the nanotube by precipitation of Ti (IV) in the inner and outer surface of the nanotubes, which fills the tube and pores.

The MAH synthesis (Figures 4c and 4d) gave homogeneous nanotubes. The tubular structures were similar in all samples, even after varying the time and temperature of synthesis. In contrast to the CH method, higher temperatures did not affect the tubular structures, including samples synthesized at 150 °C. The nanotubes had diameters around 10 to 12 nm, much smaller than those obtained with the CH method (20 to 80 nm).
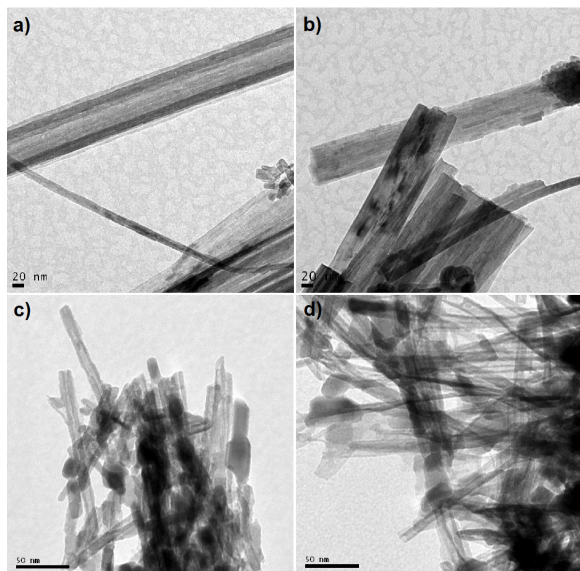

Figure 4: MET images of the samples: a) CH 110-20, b) CH 130-48, c) MAH 130-1.5 and (d) MAH 150-3.

Photocatalytic Activity

For the photocatalytic tests of nanotubes using methylene blue there was solution discoloration at time zero. This is attributed to the adsorption phenomenon. Thus, the samples were kept in the dark for 20 minutes before the start of photocatalysis.

Figure 5 presents the change in dye concentration over the initial adsorption and subsequent photo-degradation. The nanotubes possess excellent adsorption capacity and photocatalytic activity. At time zero, most nanotubes adsorbed more than 90% of the dye; after 60 minutes of photocatalysis, 99% was removed. The sample CH 130-48 reduced the dye by 76%. This sample, as shown in previous tests, has a predominantly non-tubular structure. Thus, its structural properties (smaller surface area and pore volume) may have contributed to this worse photocatalytic performance. TiO_2 P25 was used for comparison testing. It adsorbed 5% of the dye, which increased this to 96% after 60 minutes.
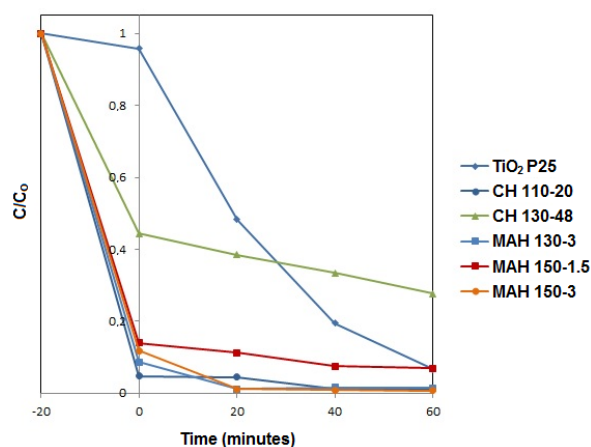

Figure 5: Photocatalysis results with TNTs and TiO_2 P25 for the removal of methylene blue.

Other photocatalytic tests for methyl orange dye were performed. In these tests, the same procedure was performed by keeping the solution in the dark for 20 minutes before the start of photocatalysis (Figure 6).

Note that the reaction does not proceed before dye adsorption and photocatalysis. All nanotubes, regardless of the method and conditions of synthesis, showed photocatalytic activity. As with methylene blue dye, nanoribbons showed lower performance and only degraded 16% of the dye in one hour. TiO_2 P25 showed slightly faster methyl orange degradation (60% in 60 minutes). The nanotubes synthesized at 150 °C by the MAH method were better and degraded 50% of the dye.

The photocatalytic activity data can be directly related to the synthesis temperature and surface area of the samples. The samples synthesized at higher temperatures (150 °C) had a higher surface area and therefore degraded the most dye. Synthesis at 150 °C was only possible by microwave. This showed the best results in the photocatalytic tests. Thus, we

concluded that a larger surface area of nanotubes caused better photocatalytic performance. In addition to the considerable reduction in synthesis time, the MAH method presented advantages such as uniform formation of nanotubes, higher temperatures of synthesis, and high surface area nanotubes.
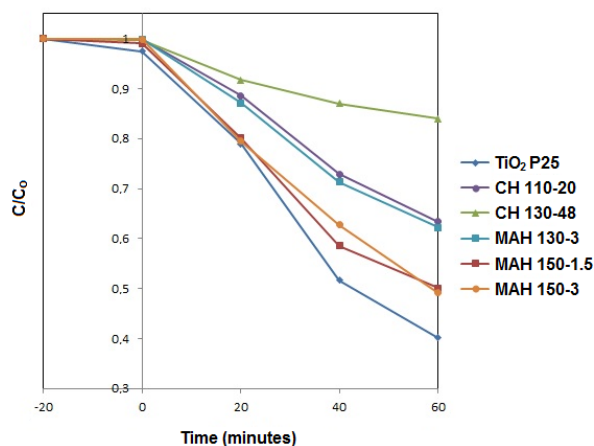

Figure 6: Photocatalysis results with TNTs and TiO_2 P25 for the removal of methyl orange.

Both the dye and the molecular structure affected the results. Methyl orange is anionic, unlike methylene blue, which is cationic. The interaction of dye molecules is not the same on the surface of the nanotubes. What differentiates TiO_2 P25 from the nanotubes is the large number of hydroxyl groups (OH^-) on their surface. Therefore, nanotubes showed a great adsorption capacity.

The hydroxyl groups present in the TiO_2 surface play an important role in the photocatalytic performance. However, the explanations are limited to the formation of a large number of hydroxyl groups on the surface of the TiO_2 nanotubes. Using infrared spectroscopy, Qian *et al*. (2006) suggested the adsorption of water molecules on the surface of the nanotubes. This generates a hydroxyl group on the surface of the nanotubes and a proton. The work of Rendón-Rivera *et al*. (2011) suggests that this water dissociation occurs due to strong deformation of the octahedron TiO_6 in the curved structure of the nanotube.

Due to its high surface area, the adsorption of a substrate becomes very favorable on the surface of the nanotubes. The work of Natarajan *et al*. (2014) used infrared data to show no change in the crystalline structure of the nanotubes. This confirms that the preferential adsorption of methylene blue dye occurs only on the surface of the nanotubes. There was no change in pH during adsorption (5.5-6.0),

indicating no ion exchange mechanism that liberates protons into solution. Thus, we can say that the preferential adsorption of methylene blue on nanotubes is due to electrostatic interactions between oppositely charged species and not ion exchange.

Methylene Blue Adsorption on TNTs

To evaluate the adsorption capacity of the TNTs, the adsorption data were fitted to Langmuir and Freundlich isotherm equations to describe the equilibrium nature of adsorption. The results of methylene blue adsorption isotherms on the TNTs are presented in Figure 7.
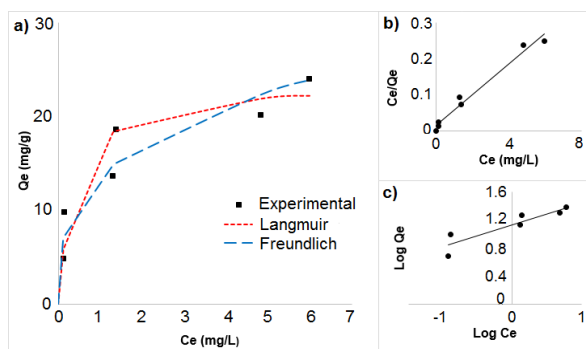

Figure 7: a) Equilibrium isotherm with Langmuir and Freundlich adsorption isotherm models for methylene blue adsorption on TNT. b) Linear plot of C_e/Q_e vs C_e. c) Linear plot of log Q_e vs log C_e.

The Langmuir isotherm model assumes that all the forces acting on the adsorption are similar in nature to those that involve a chemical reaction. It also assumes that the sorption is summed up in a single layer of substance molecules on the surface of the solid particles. The linear expression of the Langmuir isotherm (Langmuir, 1918) can be expressed by Equation (2):

$$\frac{C_e}{Q_e} = \frac{1}{Q_0 b} + \frac{C_e}{Q_e} \tag{2}$$

where Q_e is the equilibrium adsorption amount (mg/g); Q_0 is the maximum adsorption amount (mg/g); b is the adsorption constant (L/mg), and C_e is the equilibrium concentration of methylene blue (mg/L). The values of Q_0 and b for adsorption of methylene blue were calculated from the slope and intercept of a linear plot of C_e/Q_e vs C_e. The linear plots are shown in Figure 7b, and the results are tabulated in Table 4.

Table 4: Parameters of adsorption isotherm model of methylene blue on TNT.

Model	Parameters	Values
Langmuir	Q_0 (mg/g)	23.64
	b (L/mg)	2.60
	R^2	0.9747
Freundlich	K_f (mg/g)	13.63
	n	3.18
	R^2	0.8302

The Freundlich isotherm model considers that multilayer adsorption occurs and is useful to describe sorption on a highly heterogeneous surface. The linear form of the Freundlich equation (Freundlich, 1906) is given by Equation (3):

$$\log Q_e = \log K_f + \frac{1}{n \log C_e} \tag{3}$$

where K_f (mg/g) is the adsorption capacity of TNT, and n suggests the favorability of the adsorption process. The slope and intercept of the linear plot of log Q_e vs log C_e (Fig. 6c) gives the values of K_f and n (Table 4).

The results revealed that the experimental data were fitted quite well by both Langmuir and Freundlich isotherms. However, the correlation coefficient R^2 for the Langmuir isotherm model was apparently higher than that of the Freundlich model for adsorption of methylene blue.

The fact that the Langmuir isotherm fitted slightly better with the experimental data might be due to the uniform nanotubular structure of TNTs and homogeneous distribution of active sites on the walls. This indicates that monolayer adsorption occurred.

The essential characteristic of the Langmuir isotherm can also be evaluated by the dimensionless adsorption intensity R_L given by Equation (4):

$$R_L = \frac{1}{1 + bC_0} \tag{4}$$

The values of R_L at different initial concentrations of methylene blue between 0 and 1 suggest that adsorption on the surface of TNTs is favorable. In addition, the low R_L values (<0.04) implied that the interaction of methylene blue molecules with TNTs might be relatively strong (Xiong *et al*., 2010). In our experiment, the value of R_L was 0.016. Therefore, the TNTs are a good potential adsorbent for methylene blue due to their high adsorption capacity.

CONCLUSIONS

The MAH method resulted in uniform nanotubes with high surface areas. The synthesis at 150 °C was only possible via MAH. This showed the best results in the photocatalytic tests with methyl orange; it degraded up to 50% of the dye within 60 minutes. Moreover, we concluded that a larger surface area of nanotubes resulted in a better photocatalytic performance. Thus, in addition to the considerable reduction in synthesis time, the MAH method offers uniform formation of nanotubes, higher temperatures of synthesis, and higher surface area products. The methylene blue experiment showed that adsorption is the predominant phenomenon. The best-fit adsorption isotherm was achieved with the Langmuir isotherm, indicating that monolayer adsorption occurred. Therefore, the results demonstrated that TNTs could be employed as promising adsorbents or photocatalysts.

REFERENCES

Bavykin, D. V., Parmon, V. N., Lapkin, A. A., Walsh, F. C., The effect of hydrothermal conditions on the mesoporous structure of TiO_2 nanotubes. Journal of Materials Chemistry, 14, 3370-3377 (2004).

Bavykin, D. V., Friedrich, J. M., Walsh, F. C., Protonated titanates and TiO_2 nanostructured materials: Synthesis, properties and applications. Advanced Materials, 18, 2807-2824 (2006).

Chung, C. -C., Chung T. -W., Yang, T. C. -K., Rapid synthesis of titania nanowires by microwave-assisted hydrothermal treatments. Industrial & Engineering Chemistry Research, 47, 2301-2307 (2008).

Cui, L., Hui, K. N., Hui, K. S., Lee, S. K., Zhou, W., Wan, Z. P., Thuc, C. -N. H., Facile microwave-assisted hydrothermal synthesis of TiO_2 nanotubes. Materials Letters, 75, 175-178 (2012).

Ferreira, O. P., Filho, A. G. S., Filho, J. M., Alves, O. L., Unveiling the structure and composition of titanium oxide nanotubes through ion exchange chemical reactions and thermal decomposition processes. Journal of the Brazilian Chemical Society, 17, 393-402 (2006).

Freundlich, H. M. F., Uber die adsorption in losungen. The Journal of Physical Chemistry, 57, 385-470 (1906).

Hoyer, P., Formation of a titanium dioxide nanotube array. Langmuir, 12, 1411-1413 (1996).

Huang, J., Cao, Y., Huang, Q., He, H., Liu, Y., Guo, W., Hong, M., High-temperature formation of titanate nanotubes and the transformation mechanism of nanotubes into nanowires. Crystal Growth & Design, 9, 3632-3637 (2009).

Huang, K. -C., Chien, S. -H., Improved visible-light-driven photocatalytic activity of rutile/titania-nanotube composites prepared by microwave-assisted hydrothermal process. Applied Catalysis, B, Environmental, 140-141, 283-288 (2013).

Kasuga, T., Hiramatsu, M., Hoson, A., Sekino, T., Niihara, K., Formation of titanium oxide nanotube. Langmuir, 14, 3160-3163 (1998).

Kim, D., Ghicov, A., Albu, S. P., Schmuki, P., Bamboo-type TiO_2 nanotubes: Improved conversion efficiency in dye-sensitized solar cells. Journal of the American Chemical Society, 130, 16454-16455 (2008).

Ku, S. J., Jo, G. C., Bak, S. M., Kim, S. M., Shin, Y. R., Kim, K. H., Kwon, S. H., Kim, J. -B., Highly ordered freestanding titanium oxide nanotube arrays using Si-containing block copolymer lithography and atomic layer deposition. Nanotechnology, 24, 1-8 (2013).

Lachheb, H., Puzenat, E., Houas, A., Ksibi, M., Elaloui, E., Guillard, C., Herrmann, J. M., Photocatalytic degradation of various types of dyes (Alizarin S, Crocein Orange G, Methyl Red, Congo Red, Methylene Blue) in water by UV-irradiated titania. Applied Catalysis, B, Environmental, 39, 75-90 (2002).

Langmuir, I., The adsorption of gases on plane surfaces of glass, mica and platinum. Journal of the American Chemical Society, 40, 1361-1403 (1918).

Lee, N. -H., Oh, H. -J., Jung, S. -C., Lee, W. -J., Kim, D. -H., Kim, S. -J., Photocatalytic properties of nanotubular-shaped TiO_2 powders with anatase phase obtained from titanate nanotube powder through various thermal treatments. International Journal of Photoenergy, 2011, 1-7 (2011).

Li, L., Qin, X., Wang, G., Qi, L., Du, G., Hu, Z., Synthesis of anatase TiO_2 nanowires by modifying TiO_2 nanoparticles using the microwave heating method. Applied Surface Science, 257, 8006-8011 (2011).

Liu, N., Chen, X., Zhang, J., Schwank, J. W., A review on TiO_2-based nanotubes synthesized via hydrothermal method: Formation mechanism, structure modification, and photocatalytic appli-cations. Catalysis Today, 225, 34-51 (2014).

Luan, X., Wang, Y., Preparation and photocatalytic activity of Ag/bamboo-type TiO_2 nanotube composite electrodes for methylene blue degradation. Materials Science in Semiconductor Processing, 25, 43-51 (2014).

Macak, J. M., Barczuk, P. J., Tsuchiya, H., Nowakowska, M. Z., Ghicov, A., Chojak, M., Bauer, S., Virtanen, S., Kulesza, P. J., Schmuki, P., Self-organized nanotubular TiO_2 matrix as support for dispersed Pt/Ru nanoparticles: Enhancement of the electrocatalytic oxidation of methanol. Electrochemistry Communications, 7, 1417-1422 (2005).

Natarajan, T. S., Bajaj, H. C., Tayade, R. J., Preferential adsorption behavior of methylene blue dye onto surface hydroxyl group enriched TiO_2 nanotube and its photocatalytic regeneration. Journal of Colloid and Interface Science, 433, 104-114 (2014).

Peng, Y. -P., Lo, S. -L., Ou, H. -H., Lai, S. -W., Microwave-assisted hydrothermal synthesis of N-doped titanate nanotubes for visible-light-responsive photocatalysis. Journal of Hazardous Materials, 183, 754-758 (2010).

Qian, M. L., Zhang, T., Wageh, S., Jin Z. S., Du Z. L., Wang, Y. S., Xu, X. R. Study of blue electroluminescence from titania nanotubes doped into a polymeric matrix. Nanotechnology, 17, 100-104 (2006).

Rendón-Rivera, A., Toledo-Antonio, J. A., Cortés-Jácome, M. A., Angeles-Chávez, C., Generation of highly reactive OH groups at the surface of TiO_2 nanotubes. Catalysis Today, 166, 18-24 (2011).

Stylidi, M., Kondarides, D. I., Verykios, X. E., Mechanistic and kinetic study of solarlight induced photocatalytic degradation of Acid Orange 7 in aqueous TiO_2 suspensions. International Journal of Photoenergy, 5, 59-67 (2003).

Trommer, R. M., Alves, A. K., Bergmann, C. P., Synthesis, characterization and photocatalytic property of flame sprayed zinc oxide nanoparticles. Journal of Alloys and Compounds, 491, 296-300 (2010).

Tsai, C. C., Teng, H., Structural features of nanotubes synthesized from NaOH treatment on TiO_2 with different post-treatments. Chemistry of Materials, 18, 367-373 (2006).

Wu, X., Jiang, Q. -Z., Ma, Z. -F., Fu, M., Shangguan, W. -F., Synthesis of titania nanotubes by microwave irradiation. Solid State Communication, 136, 513-517 (2005).

Xiong, L., Yang, Y., Mai, J., Sun, W., Zhang, C., Wei, D., Chen, Q., Ni, J., Adsorption behavior of methylene blue onto titanate nanotubes. Chemical

Engineering Journal, 156, 313-320 (2010).

Yang, J., Jin, Z., Wang, X., Li, W., Zhang, J., Zhang, S., Guo, X., Zhang, Z., Study on composition, structure and formation process of nanotube $Na_2Ti_2O_4(OH)_2$. Dalton Transactions, 20, 3898-3901 (2003).

Yuan, S., Yu, L., Shi, L. Y., Wu, J., Fang, J. H., Zhao, Y., Highly ordered TiO_2 nanotube array as recyclable catalyst for the sonophotocatalytic degradation of methylene blue. Catalysis Communications, 10, 1188-1191 (2009).

Zhang, Z. H., Yuan, Y., Shi, G. Y., Fang, Y. J., Liang, L. H., Ding, H. C., Jin, L. T., Photoelectrocatalytic activity of highly ordered TiO_2 nanotube arrays electrode for azo dye degradation, Environmental Science & Technology, 41, 6259-6263 (2007).

Zwilling, V., Darque-Ceretti, E., Boutry-Forveille, A., David, D., Perrin, M. Y., Aucouturier, M., Structure and physicochemistry of anodic oxide films on titanium and TA6V alloy. Surface and Interface Analysis, 27, 629-637 (1999).